



# Investigation of the water exchange mechanism of the Plutonyl(VI) and Uranyl(VI) ions with quantum chemical methods

Antonio Prlj & François P. Rotzinger

**To cite this article:** Antonio Prlj & François P. Rotzinger (2015) Investigation of the water exchange mechanism of the Plutonyl(VI) and Uranyl(VI) ions with quantum chemical methods, Journal of Coordination Chemistry, 68:17-18, 3328-3339, DOI: [10.1080/00958972.2015.1059425](https://doi.org/10.1080/00958972.2015.1059425)

**To link to this article:** <http://dx.doi.org/10.1080/00958972.2015.1059425>




View supplementary material 



Accepted author version posted online: 12 Jun 2015.  
Published online: 14 Jul 2015.



Submit your article to this journal 



Article views: 90



View related articles 



View Crossmark data 

# Investigation of the water exchange mechanism of the Plutonyl(VI) and Uranyl(VI) ions with quantum chemical methods

ANTONIO PRLJ and FRANÇOIS P. ROTZINGER\*

Institut des Sciences et Ingénierie Chimiques, Ecole Polytechnique Fédérale de Lausanne (EPFL),  
Lausanne, Switzerland

(Received 27 February 2015; accepted 6 May 2015)



**Associative mechanism:**

$\Delta G^\ddagger(\text{An} = \text{Pu}) = 33\text{--}34 \text{ kJ/mol}$ ,  $\Delta G^\ddagger(\text{An} = \text{U}) = 30\text{--}37 \text{ kJ/mol}$

**Dissociative mechanism:**

$\Delta G^\ddagger(\text{An} = \text{Pu}) = 46\text{--}49 \text{ kJ/mol}$ ,  $\Delta G^\ddagger(\text{An} = \text{U}) = 52\text{--}53 \text{ kJ/mol}$

The water exchange reactions of  $[\text{PuO}_2(\text{OH}_2)_5]^{2+}$  and  $[\text{UO}_2(\text{OH}_2)_5]^{2+}$  were investigated with density functional theory (DFT) and wave function theory (WFT). Geometries and vibrational frequencies were calculated with DFT and CPCM hydration. The electronic energies were evaluated with general multiconfiguration quasi-degenerate second-order perturbation theory (GMC-QDPT2). Spin-orbit (SO) effects, computed with SO configuration interaction (SO-CI), are negligible. Both Actinyl(VI) ions react via an associative exchange mechanism, most likely  $I_a$ . The Gibbs activation energies ( $\Delta G^\ddagger$ ) at 25 °C are 33–34 and 30–37 kJ mol<sup>−1</sup> for  $[\text{PuO}_2(\text{OH}_2)_5]^{2+}$  and  $[\text{UO}_2(\text{OH}_2)_5]^{2+}$ , respectively.  $\Delta G^\ddagger$  for dissociative mechanisms ( $I_d$ ) is higher by more than 15 kJ mol<sup>−1</sup>.

**Keywords:** Actinides; Quantum chemical calculations; Reaction mechanisms; Water exchange reactions; Aqua ions

## Introduction

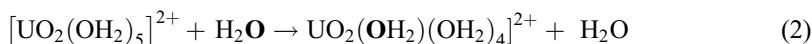
In the Plutonyl(VI) aqua ion, five water molecules are coordinated in the equatorial plane [1]. The exchange of these water molecules, reaction (1), was measured with <sup>1</sup>H NMR by Bardin *et al.* [2], whereby the rate constant extrapolated to 25 °C was estimated to be approximately 10<sup>4</sup> s<sup>−1</sup>.



\*Corresponding author. Email: [francois.rotzinger@epfl.ch](mailto:francois.rotzinger@epfl.ch)

Dedicated to Professor Rudi van Eldik on the occasion of his 70th birthday.

For the corresponding reaction (2) of the Uranyl(VI) aqua ion, they obtained the same value at 25 °C,  $10^4 \text{ s}^{-1}$ .



It is lower by about two orders of magnitude than the rate constant of  $(1.30 \pm 0.05) \times 10^6 \text{ s}^{-1}$  measured by Farkas *et al.* [3] via  $^{17}\text{O}$  NMR. In this study, erroneously [4], the dissociative (D) mechanism was attributed to reaction (2). Assuming a transmission coefficient ( $\kappa$ ) of 1, they obtained a Gibbs activation energy ( $\Delta G^\ddagger$ ) of  $38.0 \text{ kJ mol}^{-1}$ .

Later, Kerisit and Liu [5] studied reaction (2) with classical molecular dynamics (MD) simulations and determined  $\Delta G^\ddagger = 35.1 \text{ kJ mol}^{-1}$  and a transmission coefficient  $\kappa = 0.194$  via the reactive flux method (using model 1 in Ref. [5]). Based on  $\kappa = 0.194$ , Farkas *et al.*'s  $\Delta G^\ddagger$  is recalculated as  $34.0 \text{ kJ mol}^{-1}$ . Thus, Kerisit *et al.*'s and Farkas *et al.*'s data for reaction (2) agree.

The exchange mechanism of reaction (2) was attributed based on quantum chemical calculations. Among numerous studies, the most reliable ones using the most advanced quantum chemical methods and implicit solvation or the most elaborate treatment of hydration are presented. Bühl and coworkers [6, 7] performed *ab initio* MD simulations of  $[\text{UO}_2]^{2+}$  with 59  $\text{H}_2\text{O}$  molecules in a cubic box using the BLYP functional [8, 9] and periodic boundary conditions. For the associative (A) and the less favorable dissociative mechanisms, they obtained Helmholtz activation energies of  $28.0$  and  $45.2 \text{ kJ mol}^{-1}$ , respectively. In an *ab initio* molecular orbital (MO) study [4], geometries and vibrational frequencies were computed at the complete active space self-consistent field (CASSCF) level, whereby hydration was treated using the polarizable continuum model (PCM) [10, 11]. Total energies were calculated with the multiconfiguration quasi-degenerate second-order perturbation theory [12, 13], yielding Gibbs activation energies of  $35.3$  and  $57.1 \text{ kJ mol}^{-1}$  for the A and D mechanisms, respectively. The value for A is in perfect agreement with the above-mentioned experimental value and, hence, an associative mechanism operates for reaction (2).

While the water exchange rate and mechanism of Uranyl(VI) are established, this is not the case for Plutonyl(VI). Since the exchange rate constant for reaction (2) measured by Bardin *et al.* [2] is too low by a factor of about 100, the corresponding value for reaction (1) might also be inaccurate. In classical MD simulations of Actinyl ions in water, Tiwari *et al.* [14] calculated  $\Delta G^\ddagger$  for reactions (1) and (2) following the associative interchange ( $I_a$ ) pathway as  $28.7 \pm 0.8$  and  $21.0 \pm 0.1 \text{ kJ mol}^{-1}$ . Since the value for (2) is underestimated by  $13\text{--}14 \text{ kJ mol}^{-1}$ , the value of  $28.7 \text{ kJ mol}^{-1}$  for Plutonyl(VI) cannot be considered reliable without reservation. To assess the Gibbs activation energy and the mechanism of reaction (1), these two water exchange reactions were studied with density functional theory (DFT) and wave function theory (WFT).

## Computational details

Calculations were performed using the *GAMESS* [15, 16] programs. For Pu and U, Karlsruhe def-TZVP basis sets [17] without the *g* function and the corresponding small-core effective core potentials (ECP) [18] with  $Z = 60$  were used. Since *GAMESS* does not support ECP *h* functions, a modified version thereof (as given in the Supplementary Material)

was used. For O and H, modified [19] Karlsruhe def2-TZVP basis sets [20, 21] were taken. Figures 1 and 2 were generated with MacMolPlt [22].

The geometries and vibrational frequencies were computed with (spin unrestricted) DFT and hydration based on the conductor polarizable continuum model (CPCM) [10, 11, 23]. The Hessians were calculated numerically (based on analytical gradients) using the double-difference method and projected to eliminate rotational and translational contaminants [24]. A DFT grid finer than the default was taken ( $n_{\text{rad}} = 120$ ,  $n_{\text{leb}} = 770$ , or  $n_{\text{rad}} = 160$  and  $n_{\text{leb}} = 974$  for functionals involving the kinetic energy density, the respective defaults are 96 and 302). The CPCM cavity was constructed using Batsanov's [25] van der Waals radii of the atoms. A finer tessellation than the default was used ( $\text{NTSALL} = 960$ , the respective default is 60).

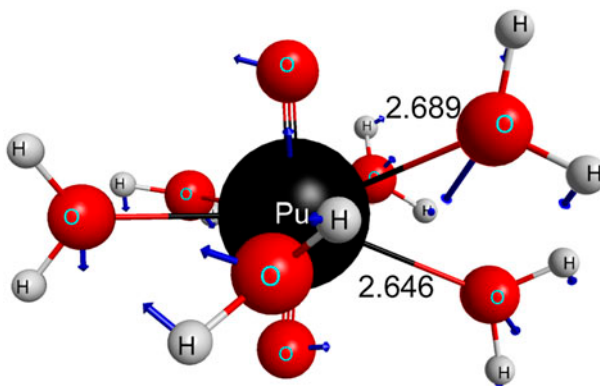


Figure 1. Structure and imaginary mode ( $66i \text{ cm}^{-1}$ ) of the TS  $[\text{PuO}_2(\text{OH}_2)_4 \cdots (\text{OH}_2)_2]^{2+ \ddagger}$  for the  $I_a$  mechanism (bond lengths in Å, LC-BOP-LRD geometry).

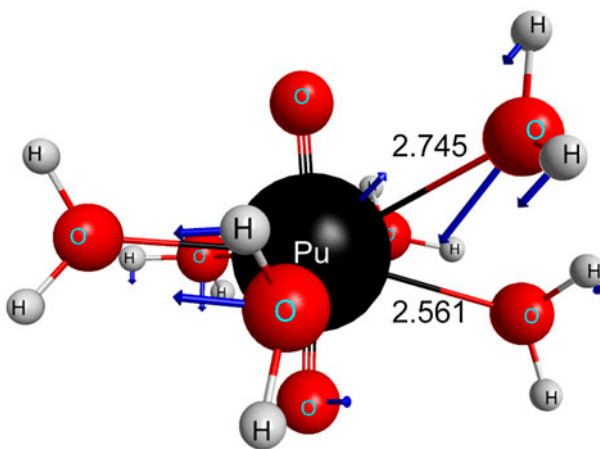


Figure 2. Structure and imaginary mode ( $33i \text{ cm}^{-1}$ ) of the TS  $[\text{PuO}_2(\text{OH}_2)_5 \cdots \text{OH}_2]^{2+ \ddagger}$  for the  $A$  mechanism (bond lengths in Å, PBE0-D3 geometry).

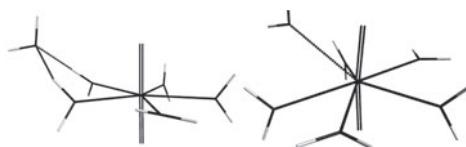
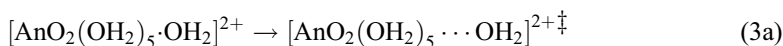
To assess the accuracy of the DFT energies, the latter were also computed with WFT using general multiconfiguration quasi-degenerate second-order perturbation theory (GMC-QDPT2) [26–29], whereby the 6s and 6p MOs of U and Pu were included in the PT2 treatment. The multiconfiguration self-consistent-field (MCSCF) and the GMC-QDPT2 calculations (with *krot* = .t., *kszdoo* = .t., and *thrde* = 0) were based on the occupationally restricted multiple active space (ORMAS) [30] technique to realize a maximum excitation level of two within the MCSCF active space. For the Uranyl complexes and the water molecule, active spaces with two sub-spaces, denoted [19] as (10–12/6,0–2/6,12) and (6–8/4,0–2/4,8), respectively (space 1, 10–12/6: minimum number of electrons–maximum number of electrons/number of MOs, space 2, 0–2/6: as for space 1, last number, 12: total number of electrons), were used. For the Plutonyl complexes exhibiting two unpaired electrons, the active space, (10–12/6,0–4/2,0–2/6,14), contained three sub-spaces and 14 electrons. The spin-orbit (SO) energy was calculated based on the MCSCF wave function with SO configuration interaction (SO–CI) involving three singlet and one triplet states (with an active space of two electrons in the  $2f_{\delta}$  MOs). The full Breit-Pauli Hamiltonian including a partial two-electron operator [31–33] was used. The CPCM hydration energy was obtained from the MCSCF calculations.

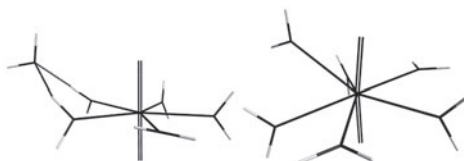
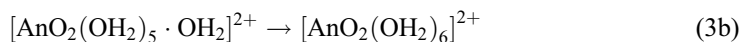
The transition states (TS) were located by maximizing the energy along the reaction coordinate (the imaginary mode) via eigenmode following. They exhibited a single imaginary frequency. Reactants, products, and intermediates were obtained via computation of the intrinsic reaction coordinate. All of their computed vibrational frequencies were real. Selected atomic coordinates of the investigated species are given in tables S1–S15 (see online supplemental material at <http://dx.doi.org/10.1080/00958972.2015.1059425>).

### Methods for the calculation of the Gibbs activation energy ( $\Delta G^{\ddagger}$ ) for associative and dissociative exchange mechanisms

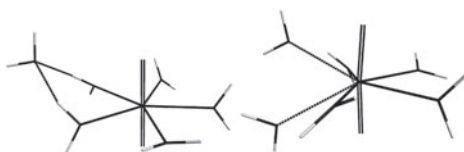
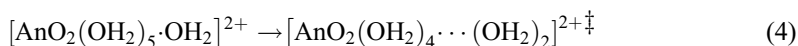
The water exchange reactions (1) and (2) can be formulated as unimolecular processes using water-adducts [34–36]. Alternatively, the reactions may involve a water molecule from the bulk solution.

Using water-adducts, denoted as  $[\text{AnO}_2(\text{OH}_2)_5 \cdot \text{OH}_2]^{2+}$  (“ $\cdot \text{OH}_2$ ” representing water in the second coordination sphere), the Gibbs activation energy ( $\Delta G^{\ddagger}$ ) for the associative (A) mechanism [37–39] is available via equation (3) (An=Pu, U), whereby equation (3b) describes the formation of the intermediate for A. Weak bonds in the TS are represented by “...”.

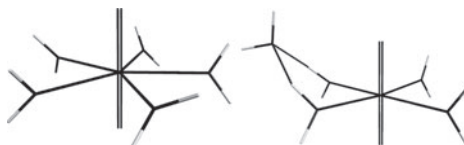
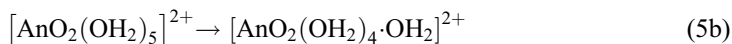
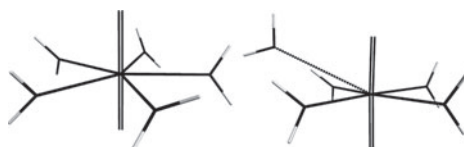
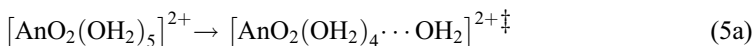




Equation (4) represents the interchange mechanisms  $I_a$ ,  $I$  or  $I_d$  [37–39]. Their TSs exhibit two weak bonds.



Solvent molecules are not involved in the activation step of the dissociative (D) pathway (5a) [37–39], but a water molecule is eliminated in the formation of the respective intermediate (5b).

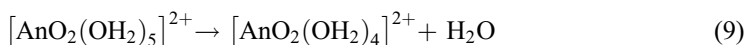
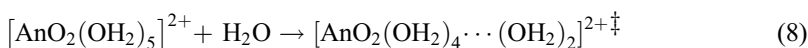
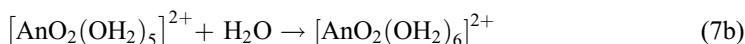
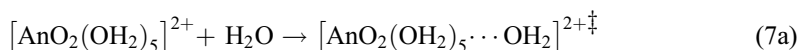


$\Delta G^\ddagger$  is calculated using equation (6):

$$\Delta G^\ddagger = \Delta E^\ddagger + \Delta G_{\text{solv}}^\ddagger + \Delta g^{\circ\ddagger} \quad (6)$$

$\Delta E^\ddagger$  is the electronic activation energy in the gas phase,  $\Delta G_{\text{solv}}^\ddagger$  is the difference in solvation energies, and  $\Delta g^{\circ\ddagger}$  is the difference of the thermal corrections to the Gibbs energy (including the zero point energy) at 1 atm and 25 °C.  $\Delta E^\ddagger$  and  $\Delta G_{\text{solv}}^\ddagger$  are calculated at the geometries of the solvated species and  $\Delta g^{\circ\ddagger}$  is based on the vibrational frequencies of the solvated species.  $\Delta G$  for reactions (3b) and (5b) is calculated analogously.

As already mentioned, bulk solvent molecules are not involved in reaction (5a). The other reactions, (3), (4) and (5b), are rewritten to take into account the participation of water from the bulk solvent:



Reactions (7), (8) and (9) are not unimolecular. Therefore, equation (6) cannot be used for the calculation of  $\Delta G^\ddagger$  and  $\Delta G$  without corrections for the standard states in the gas phase (1 atm) and solution (1 M). For reactions (7) and (8),  $\Delta G^\ddagger$  is obtained via equation (10) [40]:

$$\Delta G^\ddagger = \Delta E^\ddagger + \Delta G_{\text{solv}}^\ddagger + \Delta g^\ddagger - RT(\ln(V^\circ/V^*) + \ln[\text{H}_2\text{O}]) \quad (10)$$

$V^\circ$  is the volume of 1 mol (ideal gas) at 1 atm and 25 °C, and  $V^*$  is equal to one liter. Because the concentration of the water solvent is not 1 M, the  $RT \ln[\text{H}_2\text{O}]$  term is also required. Since a water molecule is liberated in equation (9), the corrections have the opposite sign, and  $\Delta G$  has to be evaluated via equation (11):

$$\Delta G = \Delta E + \Delta G_{\text{solv}} + \Delta g^\circ + RT(\ln(V^\circ/V^*) + \ln[\text{H}_2\text{O}]) \quad (11)$$

Both methods exhibit strengths and limitations. With water-adducts, all of the reactions are unimolecular. Hence, no corrections for the various standard states are required. The differences in electronic energies correspond approximately to those of the Gibbs energies. As a disadvantage, the number of isomers is larger for the water-adducts. Therefore, elucidation of the global minimum is more demanding. Furthermore, the bridged structures of the water-adducts do not correspond to the structures in solution, and the reactants for the A,  $I_a$ , I, and  $I_d$  mechanisms differ from that for D. For the reactions with water from the bulk solution, corrections for the different standard states in the gas phase and solution are required, and the solvent concentration has to be taken into account as well. The gas phase electronic energy differences may differ strongly from the corresponding Gibbs energy differences in solution. As a benefit, all of the mechanisms are tractable starting with the same reactant structure.

In this study, reactions (1) and (2) were investigated using both methods.

Results and discussion

Geometry of the reactants

The geometries and vibrational frequencies of all the species involved in reaction (1) were computed with various functionals, whereby some of them contain Grimme’s dispersion correction (D3) [41]. The geometry of the reactant  $[\text{PuO}_2(\text{OH}_2)_5]^{2+}$  was optimized with PBE0-D3 [41–44], LC-BOP-LRD [45, 46],  $\omega$ B97X [47, 48], TPSSh [49, 50], TPSSh-D3 [41, 49, 50] and LC-BLYP [51]. TPSSh and TPSSh-D3 yielded Pu=O bond lengths (table 1), closest to experiment [52] (1.759 Å), and all of the presently used functionals reproduced the experimental Pu–O(H<sub>2</sub>) bond lengths of 2.42 Å within 0.02 Å. The errors in the vibrational O=Pu=O frequencies follow the same trend. For the  $[\text{UO}_2(\text{OH}_2)_5]^{2+}$  reactant, the three functionals PBE0-D3, LC-BOP-LRD, and  $\omega$ B97X gave rise to too short U=O bonds (table 2), and the U–O(H<sub>2</sub>) bonds were slightly too long compared with experiment [56]. The too short Pu=O and U=O bond lengths together with the too high O=An=O (An=Pu, U) frequencies arise from the inaccurate treatment of static correlation [4, 59–61] with DFT.

In the TS for D, the average An–O(H<sub>2</sub>) bonds are shortened by ~0.05 Å, whereas in that for A, they are elongated by about the same amount. In the TS for *I*<sub>a</sub>, the elongation of the

Table 1. Pu=O and Pu–O(H<sub>2</sub>) bond lengths and O=Pu=O vibrational frequencies of the reactant  $[\text{PuO}_2(\text{OH}_2)_5]^{2+}$  (experimental data obtained in aqueous solutions).

	$d(\text{Pu}=\text{O})$ , Å	$d(\text{Pu}-\text{O}(\text{H}_2))^a$ , Å	$\nu_s$ , cm <sup>−1</sup>	$\nu_{as}$ , cm <sup>−1</sup>
EXAFS <sup>b</sup>	1.759 ± 0.005	2.42 ± 0.01	835, 833	962
Raman <sup>c,d</sup>				
IR <sup>e</sup>				
LC-BOP-LRD	1.680	2.415	1016	1081
$\omega$ B97X	1.693	2.438	971	1045
PBE0-D3	1.702	2.415	936	1024
TPSSh	1.727	2.414	877	974
TPSSh-D3	1.726	2.413	879	976
LC-BLYP	1.707	2.391	942	1024

<sup>a</sup>Average of the 5 Pu–O(H<sub>2</sub>) bond lengths.

<sup>b</sup>Ref. [52].

<sup>c</sup>Ref. [53].

<sup>d</sup>Ref. [54].

<sup>e</sup>Ref. [55].

Table 2. U=O and U–O(H<sub>2</sub>) bond lengths and O=U=O vibrational frequencies of the reactant  $[\text{UO}_2(\text{OH}_2)_5]^{2+}$  (experimental data obtained in aqueous solutions).

	$d(\text{U}=\text{O})$ , Å	$d(\text{U}-\text{O}(\text{H}_2))^a$ , Å	$\nu_s$ , cm <sup>−1</sup>	$\nu_{as}$ , cm <sup>−1</sup>
EXAFS <sup>b</sup>	1.76	2.41	869, 872, 874	962.5, 965
Raman <sup>c,d,e</sup>				
IR <sup>e,f</sup>				
LC-BOP-LRD	1.722	2.437	1006	1041
$\omega$ B97X	1.732	2.455	972	1013
PBE0-D3	1.739	2.432	948	999

<sup>a</sup>Average of the 5 U–O(H<sub>2</sub>) bond lengths.

<sup>b</sup>Ref. [56].

<sup>c</sup>Ref. [57].

<sup>d</sup>Ref. [53].

<sup>e</sup>Ref. [58].

<sup>f</sup>Ref. [55].



Pu–O(H<sub>2</sub>) bonds is smaller (~0.025 Å). Upon activation, the An=O bond length changes follow the same trend, but with much smaller variations (by ±0.002 Å for Pu and ±0.003 Å for U). The bond lengths in the *I*<sub>a</sub>, A, and D TSs are given in table S16 (Supplementary Material).

### Gibbs activation energies ( $\Delta G^\ddagger$ ) for associative and dissociative water exchange mechanisms

To assess the accuracy of the above-mentioned functionals, Gibbs activation energies (table 3) for associative and dissociative water exchange mechanisms of reaction (1) were computed at the DFT geometries with DFT and WFT. Due to the presence of static correlation in Actinyl complexes, multiconfiguration methods are required [4, 60, 61]. Thus,  $\Delta E^\ddagger$  and  $\Delta G_{\text{solv}}^\ddagger$  in equations 6, 10 and 11 ( $\Delta E$  and  $\Delta G_{\text{solv}}$  for the intermediates) were computed with DFT and GMC-QDPT2 and SO–CI (Computational Details), whereby the SO energy differences were negligible (<0.01 kJ mol<sup>−1</sup>) because both of the  $f_{\delta}$  levels are occupied by a single electron and because of the absence of low-lying triplet and singlet (excited) states. WFT hydration was calculated with MCSCF and CPCM hydration.  $\Delta G^{\circ\ddagger}$  or  $\Delta G^\circ$  was always computed with DFT (because the geometries were optimized with DFT). The relative Gibbs energy ( $\Delta G$ ) of the intermediates for the A and the D pathways with an increased or a reduced coordination number are also included in table 3. It should be noted that the LC-BOP-LRD and the ωB97X functionals yielded TS for the *I*<sub>a</sub> mechanism (figure 1), whereas with the other functionals, PBE0-D3, TPSSh, TPSSh-D3, and LC-BLYP, TSs for the A pathway (figure 2) were obtained.  $\Delta G^\ddagger$  for A is somewhat higher than for *I*<sub>a</sub>. The distinction of the A from the *I*<sub>a</sub>, and the D from the *I*<sub>d</sub> mechanisms is very demanding [4, 36]; this issue will be discussed later. For the D mechanism, WFT and DFT yielded considerably different

Table 3. Gibbs activation energy ( $\Delta G^\ddagger$ ) for the water exchange of [PuO<sub>2</sub>(OH<sub>2</sub>)<sub>5</sub>]<sup>2+</sup> <sup>a</sup>.

Mechanism	Geometry	DFT		WFT		Eq(s)
		$\Delta G^\ddagger$	$\Delta G$	$\Delta G^\ddagger$	$\Delta G$	
<i>I</i> <sub>a</sub>	LC-BOP-LRD	37.9		33.6		4, 6
		31.8		33.2		8, 10
	ωB97X	34.9		35.9		4, 6
		25.8		33.5		8, 10
A	PBE0-D3	44.0	41.6	42.2	40.2	3a, 3b, 6
		27.4	24.9	36.0	34.0	7a, 7b, 10
	TPSSh	36.2	37.7	31.7	34.0	3a, 3b, 6
	TPSSh-D3	39.8	38.8	38.6	40.1	3a, 3b, 6
		33.6	32.6	42.8	44.3	7a, 7b, 10
	LC-BLYP	47.0	37.7	44.0	36.7	3a, 3b, 6
D	PBE0-D3	36.3	26.0	44.4	37.3	5a, 5b, 6
		36.3	37.7	44.4	38.0	5a, 9, 11
	LC-BOP-LRD	43.2	33.5	48.7	41.0	5a, 5b, 6
		43.2	42.9	48.7	44.9	5a, 9, 11
	ωB97X	38.8	31.0	46.3	37.8	5a, 5b, 6
		38.8	41.6	46.3	41.9	5a, 9, 11
	TPSSh	34.0	23.2	48.0	43.0	5a, 5b, 6
	TPSSh-D3	38.8	29.5	47.2	42.3	5a, 5b, 6
		38.8	45.0	47.2	45.5	5a, 9, 11
	LC-BLYP	38.0	19.9	49.9	37.1	5a, 5b, 6

<sup>a</sup>Units: kJ mol<sup>−1</sup>. Italic values indicate that the concerted mechanism might operate, since  $\Delta G > \Delta G^\ddagger$ .

$\Delta G^\ddagger$  values. The differences are smallest for LC-BOP-LRD and  $\omega$ B97X. Virtually the same differences (within  $1 \text{ kJ mol}^{-1}$ ) were observed for the corresponding electronic energy differences ( $\Delta E^\ddagger$  and  $\Delta E$ ) in the gas phase. Hence, these differences are not due to errors in the CPCM hydration. For the  $I_a$  and the A mechanisms, the WFT-DFT differences in  $\Delta G^\ddagger$  are smaller. For all of the investigated mechanisms, D,  $I_a$ , and A, the best  $\Delta G^\ddagger/\Delta G$  and  $\Delta E^\ddagger/\Delta E$  agreement was obtained with LC-BOP-LRD, followed by  $\omega$ B97X.

While the computed  $\Delta G^\ddagger$  values based on DFT do not allow the attribution of the exchange mechanism of reaction (1), WFT clearly shows that  $\Delta G^\ddagger$  for  $I_a$  and A is lower than for D (table 3). For the most reliable functionals LC-BOP-LRD and  $\omega$ B97X,  $I_a$  is favored over D by  $> 15 \text{ kJ mol}^{-1}$ .  $\Delta G^\ddagger$  for  $I_a$  and A, and  $\Delta G$  for A and D were evaluated based on both methods, that involving the water-adducts, equations (3)–(5), and the other one with the participation of water from the bulk solution, equations (5a), (7)–(9). ( $\Delta G^\ddagger$  for D does not involve water from the bulk solution). For the  $I_a$  and the A mechanisms,  $\Delta G^\ddagger$  calculated using both of these methods differs considerably for some functionals. The same holds for  $\Delta G$  for D. It is noteworthy that in the water-adducts, there are two hydrogen bonds, which, in general, are difficult to treat accurately with DFT [62].

The intermediates for the A and the D mechanisms should exhibit a lower Gibbs energy than the corresponding TSs. This is, however, not always the case (table 3) because of the approximations in the calculation of  $\Delta G^\ddagger$  and  $\Delta G$ . These are for example the geometry optimizations, for which the electronic energy is minimized for the rigid species at 0 K (not  $G$  at  $25^\circ\text{C}$ ), the equations of statistical mechanics, which were derived for the free species in the gas phase (although the vibrational frequencies of the solvated species were used for the calculation of  $\Delta g^{\circ\ddagger}$  and  $\Delta g^\circ$ ), the neglected variations of the thermodynamic properties of the bulk solvent as well as specific solute–solvent interactions, and the harmonic approximation. In cases with a small Gibbs energy difference between TS and intermediate, which gives a hypothetical life-time of the intermediate being smaller than the duration of the vibration leading to the reactant or the intermediate, the mechanism would be rather  $I_a$  or  $I_d$  than A or D [4]. Thus, for the italicized entries in table 3, for which the intermediate exhibits a higher energy than the corresponding TS, and for the entries with small  $\Delta G^\ddagger - \Delta G$  differences as well, the  $I_a$  or the  $I_d$  mechanism might operate instead of A or D.

As mentioned above and in previous work [4, 36], the distinction of the concerted ( $I_a$ ,  $I_d$ ) from the step-wise (A, D) mechanisms is subtle. For reaction (1), depending on the functional, TSs for the  $I_a$  (figure 1) and the A (figure 2) mechanisms were obtained (table 3).

Table 4. Gibbs activation energy ( $\Delta G^\ddagger$ ) for the water exchange of  $[\text{UO}_2(\text{OH}_2)_5]^{2+}$  <sup>a</sup>.

Mechanism	Geometry	DFT		WFT		Eq(s)
		$\Delta G^\ddagger$	$\Delta G$	$\Delta G^\ddagger$	$\Delta G$	
A	LC-BOP-LRD	37.5	35.8	37.2	36.0	3a, 3b, 6
		24.8	23.1	30.3	29.1	7a, 7b, 10
	$\omega$ B97X	28.3	32.9	31.0	35.8	3a, 3b, 6
		20.9	25.5	29.8	34.6	7a, 7b, 10
D	LC-BOP-LRD	47.4	21.5	52.5	27.6	5a, 5b, 6
		47.4	44.0	52.5	45.0	5a, 9, 11
	$\omega$ B97X	44.0	25.0	51.6	28.5	5a, 5b, 6
		44.0	45.7	51.6	46.1	5a, 9, 11

<sup>a</sup>Units:  $\text{kJ mol}^{-1}$ . Italic values indicate that the concerted mechanism might operate, since  $\Delta G > \Delta G^\ddagger$ .

They differ in the geometry and the imaginary mode: The TS for  $I_a$  exhibits two elongated Pu–O(H<sub>2</sub>) bonds of similar lengths (within 0.04 Å), whereas in the TS for A, the corresponding bond lengths differ by almost 0.2 Å. Furthermore, the imaginary mode of  $I_a$  describes the concerted entry and leaving of H<sub>2</sub>O ligands in contrast to the mode of A describing solely the entry of a H<sub>2</sub>O ligand. Due to the lower  $\Delta G^\ddagger$  for  $I_a$  and the small or even negative  $\Delta G^\ddagger - \Delta G$  difference for A, it is preferable to attribute the  $I_a$  mechanism to reaction (1).

As already seen,  $\Delta G^\ddagger$  and  $\Delta G$  based on DFT are not reliable and DFT does not predict the preference for an associative mechanism of reaction (1) unequivocally. In Actinyl(VI) complexes, static electron correlation is present; its appropriate treatment [4, 59–61] is mandatory to obtain reliable results. For reaction (1), the most reliable data were obtained with LC-BOP-LRD or  $\omega$ B97X geometries and frequencies, and GMC-QDPT2/SO–CI energies. Hence,  $\Delta G^\ddagger$  for the  $I_a$  and the unfavorable D or  $I_d$  mechanisms is 33–34 and 46–49 kJ mol<sup>−1</sup>, respectively.

To assess the accuracy of the present computations, the well-studied Uranyl(VI) water exchange reaction (Introduction) was re-investigated using the most accurate functionals LC-BOP-LRD and  $\omega$ B97X, and GMC-QDPT2 (table 4).  $\Delta G^\ddagger$  calculated with DFT is inaccurate and lower than  $\Delta G^\ddagger$  based on WFT, which amounts to 30–37 kJ mol<sup>−1</sup> (table 4) for the A mechanism. This value agrees with the experimental value of 34–35 kJ mol<sup>−1</sup> (Introduction). The D mechanism, exhibiting a higher  $\Delta G^\ddagger$  (by > 15 kJ mol<sup>−1</sup>), is unfavorable. Also for this reaction (2), it is preferable to attribute the  $I_a$  mechanism due to the small (LC-BOP-LRD/WFT) or negative ( $\omega$ B97X/WFT)  $\Delta G^\ddagger - \Delta G$  difference. This mechanism was also attributed by Kerisit and Liu based on classical MD simulations [5].

## Summary

The water exchange reactions of the  $f^0$  and  $f^2$  Actinyl(VI) aqua ions of U and Pu, respectively, proceed via an associative mechanism, most likely  $I_a$ . For both reactions,  $\Delta G^\ddagger$  is virtually equal (30–37 kJ mol<sup>−1</sup> for U and 33–34 kJ mol<sup>−1</sup> for Pu). For the unfavorable D pathway,  $\Delta G^\ddagger$  is higher by more than 15 kJ mol<sup>−1</sup> for both Actinyl(VI) ions. The reactivity (mechanism and  $\Delta G^\ddagger$ ) of these two ions is equal in spite of their disparate, but symmetric  $f$  orbital occupations (the occupation is asymmetric in  $f^1$  and  $f^3$  systems).

The An=O bond lengths calculated with DFT are somewhat too short for most functionals because of an imperfect treatment of static correlation. Furthermore, DFT is often inaccurate for hydrogen bonding. Therefore, the computed  $\Delta G^\ddagger$  and  $\Delta G$  are also inaccurate. In such cases, reliable results can be obtained with state-of-the-art WFT. In systems exhibiting static correlation, the adequacy of DFT and MP2 should be assessed with WFT.

Reactions involving a solvent molecule from the bulk can be treated with or without water-adducts, provided that the various standard states are taken into account.

## Supplementary material

Modified ECPs for U and Pu. Atomic coordinates of the reactants, TSs, and intermediates for the  $I_a$ , A, and D mechanisms. An=O, An–O(H<sub>2</sub>), and An···O(H<sub>2</sub>) bond lengths in the  $I_a$ , A, and D TSs (An=Pu, U).

## Acknowledgement

Some of the computations were performed by Dr B. Bertsche.

## Disclosure statement

No potential conflict of interest was reported by the authors.

## Funding

This work was supported by the Swiss National Science foundation [grant number 137666].

## References

- [1] S.O. Odoh, E.J. Bylaska, W.A. de Jong. *J. Phys. Chem. A*, **117**, 12256 (2013).
- [2] N. Bardin, P. Rubini, C. Madic. *Radiochim. Acta*, **83**, 189 (1998).
- [3] I. Farkas, I. Bányai, Z. Szabó, U. Wahlgren, I. Grenthe. *Inorg. Chem.*, **39**, 799 (2000).
- [4] F.P. Rotzinger. *Chem. Eur. J.*, **13**, 800 (2007).
- [5] S. Kerisit, C. Liu. *J. Phys. Chem. A*, **117**, 6421 (2013).
- [6] M. Bühl, R. Diss, G. Wipff. *J. Am. Chem. Soc.*, **127**, 13506 (2005).
- [7] M. Bühl, H. Kabrede. *Inorg. Chem.*, **45**, 3834 (2006).
- [8] A.D. Becke. *Phys. Rev. A*, **38**, 3098 (1988).
- [9] C. Lee, W. Yang. *Phys. Rev. B*, **37**, 785 (1988).
- [10] J. Tomasi, B. Mennucci, R. Cammi. *Chem. Rev.*, **105**, 2999 (2005).
- [11] J. Tomasi. *Theor. Chem. Acc.*, **112**, 184 (2004).
- [12] H. Nakano. *J. Chem. Phys.*, **99**, 7983 (1993).
- [13] H. Nakano. *Chem. Phys. Lett.*, **207**, 372 (1993).
- [14] S.P. Tiwari, N. Rai, E.J. Maginn. *Phys. Chem. Chem. Phys.*, **16**, 8060 (2014).
- [15] M.W. Schmidt, K.K. Baldridge, J.A. Boatz, S.T. Elbert, M.S. Gordon, J.H. Jensen, S. Koseki, N. Matsunaga, K.A. Nguyen, S.J. Su, T.L. Windus, M. Dupuis, J.A. Montgomery. *J. Comput. Chem.*, **14**, 1347 (1993).
- [16] M.S. Gordon, M.W. Schmidt, In *Theory and Applications of Computational Chemistry: The First Forty Years*, C.E. Dykstra, G. Frenking, K.S. Kim, G.E. Scuseria (Eds.), p. 1167–1189, Elsevier: Amsterdam (2005).
- [17] W. Küchle, M. Dolg, H. Stoll, H. Preuss. *J. Chem. Phys.*, **100**, 7535 (1994).
- [18] X. Cao, M. Dolg, H. Stoll. *J. Chem. Phys.*, **118**, 487 (2003).
- [19] F.P. Rotzinger. *Inorg. Chem.*, **53**, 9923 (2014).
- [20] A. Schäfer, C. Huber, R. Ahlrichs. *J. Chem. Chem.*, **100**, 5829 (1994).
- [21] F. Weigend, R. Ahlrichs. *Phys. Chem. Chem. Phys.*, **7**, 3297 (2005).
- [22] B.M. Bode, M.S. Gordon. *J. Mol. Graphics Modell.*, **16**, 133 (1998).
- [23] V. Barone, M. Cossi. *J. Phys. Chem. A*, **102**, 1995 (1998).
- [24] W.H. Miller, N.C. Handy, J.E. Adams. *J. Chem. Phys.*, **72**, 99 (1980).
- [25] S.S. Batsanov. *Inorg. Mater.*, **37**, 871 (2001).
- [26] H. Nakano, R. Uchiyama, K. Hirao. *J. Comput. Chem.*, **23**, 1166 (2002).
- [27] M. Miyajima, Y. Watanabe, H. Nakano. *J. Chem. Phys.*, **124**, 044101 (2006).
- [28] R. Ebisuzaki, Y. Watanabe, H. Nakano. *Chem. Phys. Lett.*, **442**, 164 (2007).
- [29] L. Roskop, M.S. Gordon. *J. Chem. Phys.*, **135**, 044101 (2011).
- [30] J. Ivanic. *J. Chem. Phys.*, **119**, 9364 (2003).
- [31] T.R. Furlani, H.F. King. *J. Chem. Phys.*, **82**, 5577 (1985).
- [32] H.F. King, T.R. Furlani. *J. Comput. Chem.*, **9**, 771 (1988).
- [33] D.G. Fedorov, M.S. Gordon. *J. Chem. Phys.*, **112**, 5611 (2000).
- [34] F.P. Rotzinger. *J. Am. Chem. Soc.*, **118**, 6760 (1996).
- [35] F.P. Rotzinger. *J. Am. Chem. Soc.*, **119**, 5230 (1997).
- [36] F.P. Rotzinger. *Chem. Rev.*, **105**, 2003 (2005).
- [37] C.H. Langford, H.B. Gray. *Ligand Substitution Processes*, W. A. Benjamin Inc, New York (1965).
- [38] A.E. Merbach. *Pure Appl. Chem.*, **54**, 1479 (1982).
- [39] A.E. Merbach. *Pure Appl. Chem.*, **59**, 161 (1987).
- [40] J.R. Pliego Jr, J.M. Riveros. *J. Phys. Chem. A*, **105**, 7241 (2001).

- [41] S. Grimme, J. Antony, S. Ehrlich, H. Krieg. *J. Chem. Phys.*, **132**, 154104 (2010).
- [42] J.P. Perdew, K. Burke, M. Ernzerhof. *Phys. Rev. Lett.*, **77**, 3865 (1996).
- [43] J.P. Perdew, K. Burke, M. Ernzerhof. *Phys. Rev. Lett.*, **78**, 1396 (1997).
- [44] C. Adamo, V. Barone. *J. Chem. Phys.*, **110**, 6158 (1999).
- [45] T. Sato, H. Nakai. *J. Chem. Phys.*, **131**, 224104 (2009).
- [46] T. Sato, H. Nakai. *J. Chem. Phys.*, **133**, 194101 (2010).
- [47] J.-D. Chai, M. Head-Gordon. *J. Chem. Phys.*, **128**, 084106 (2004).
- [48] J.-D. Chai, M. Head-Gordon. *Phys. Chem. Chem. Phys.*, **10**, 6615 (2008).
- [49] V.N. Staroverov, G.E. Scuseria, J. Tao, J.P. Perdew. *J. Chem. Phys.*, **119**, 12129 (2003).
- [50] V.N. Staroverov, G.E. Scuseria, J. Tao, J.P. Perdew. *J. Chem. Phys.*, **121**, 11507 (2004).
- [51] Y. Tawada, T. Tsuneda, S. Yanagisawa, T. Yanai, K. Hirao. *J. Chem. Phys.*, **120**, 8425 (2004).
- [52] P.J. Panak, C.H. Booth, D.L. Caulder, J.J. Bucher, D.K. Shuh, H. Nitsche. *Radiochim. Acta*, **90**, 315 (2002).
- [53] L.J. Basile, J.C. Sullivan, J.R. Ferraro, P. LaBonville. *Appl. Spectrosc.*, **28**, 142 (1974).
- [54] C. Madic, G.M. Begun, D.E. Hobart, R.L. Hahn. *Inorg. Chem.*, **23**, 1914 (1984).
- [55] L.H. Jones, R.A. Penneman. *J. Chem. Phys.*, **21**, 542 (1953).
- [56] C. Hennig, J. Tutschku, A. Rossberg, G. Bernhard, A.C. Scheinost. *Inorg. Chem.*, **44**, 6655 (2005).
- [57] L.M. Toth, G.M. Begun. *J. Phys. Chem.*, **85**, 547 (1981).
- [58] M. Gál, P.L. Goggin, J. Mink. *Spectrochim. Acta, Part A*, **48**, 121 (1992).
- [59] V. Vallet, U. Wahlgren, I. Grenthe. *Chem. Eur. J.*, **13**, 10294 (2007).
- [60] F.P. Rotzinger. *Chem. Eur. J.*, **13**, 10298 (2007).
- [61] L. Gagliardi. *Int. J. Quantum Chem.*, **111**, 3302 (2011).
- [62] B. Chan, A.T.B. Gilbert, P.M.W. Gill, L. Radom. *J. Chem. Theory Comput.*, **10**, 3777 (2014).